Spectral response of plasmon resonant nanoparticles with a non-regular shape

Jörg P. Kottmann and Olivier J.F. Martin

Electromagnetic Fields and Microwave Electronics Laboratory
Swiss Federal Institute of Technology, ETH–Zentrum,
8092 Zurich, Switzerland

kottmann@ifh.ee.ethz.ch,martin@ifh.ee.ethz.ch

David R. Smith and Sheldon Schultz

Department of Physics, University of California, San Diego,
9500 Gilman Drive, La Jolla, California 92093-0319, U.S.A.

Abstract: We study the plasmon resonances of $10-100\,(\mathrm{nm})$ two-dimensional metal particles with a non-regular shape. Movies illustrate the spectral response of such particles in the optical range. Contrary to particles with a simple shape (cylinder, ellipse) non-regular particles exhibit many distinct resonances over a large spectral range. At resonance frequencies, extremely large enhancements of the electromagnetic fields occur near the surface of the particle, with amplitudes several hundred-fold that of the incident field. Implications of these strong and localized fields for nano-optics and surface enhanced Raman scattering (SERS) are also discussed.

OCIS codes: (160.3900) Metals; (240.5420) Polaritons; (260.3910) Metals, optics of; (290.0290) Scattering; (260.5740) Resonance; (290.5860) Raman scattering; (330.1690) Color; (350.3950) Micro-optics; (350.4990) Particles.

References and links

1. Olivier J.F. Martin's group home page: http://www.ifh.ee.ethz.ch/~martin
2. H. Metiu, "Surface enhanced spectroscopy," Prog. Surf. Sci. **17**, 153–320 (1984).
3. M. Moskovits, "Surface-enhanced spectroscopy," Rev. Mod. Phys. **57**, 783–826 (1985).
4. K. Kneipp *et al.*, "Single molecule detection using surface-enhanced Raman scattering," Phys. Rev. Lett. **78**, 1667–1670 (1997).
5. S. Nie and S. R. Emory, "Probing single molecules and single nanoparticles by surface-enhanced Raman scattering," Science **275**, 1102–1106 (1997).
6. F. J. García-Vidal and J. B. Pendry, "Collective theory for surface enhanced Raman scattering," Phys. Rev. Lett. **77**, 1163–1166 (1996).
7. F. J. García-Vidal, J. M. Pitarke and J. B. Pendry, "Silver-filled carbon nanotubes used as spectroscopic enhancers," Phys. Rev. B **58**, 6783–6786 (1998).
8. O.J.F. Martin and C. Girard, "Controlling and tuning strong optical field gradients at a local probe microscope tip apex," Appl. Phys. Lett. **70**, 705–707 (1997).
9. W.-H. Yang, G. C. Schatz and R. P. van Duyne, "Discrete dipole approximation for calculating extinction and Raman intensities for small particles with arbitrary shape," J. Chem. Phys. **103**, 1–20 (1995).
10. T. R. Jensen, G. C. Schatz and R. P. van Duyne, "Nanosphere lithography: surface plasmon resonance spectrum . . . ," J. Phys. Chem. B **103**, 2394–2401 (1999).
11. C. F. Bohren and D. R. Huffman, *Absorption and scattering of light by small particles*, Chapter 12 (John Wiley and Sons, New York, 1983).
12. K. Bromann *et al.*, "Controlled deposition of size-selected solver nanoclusters," Science **274**, 956–958 (1996).
13. D. M. Kolb, R. Ullmann and T. Will, "Nanofabrication of small copper clusters on gold(111) electrodes by a scanning tunneling microscope," Science **275**, 1097–1099 (1996).

#21116 - $15.00 US
Received April 14, 2000; Revised May 18, 2000

14. J. Bosbach *et al.*, "Laser-based method for fabricating monodispersive metallic nanoparticles," Appl. Phys. Lett. **74**, 2605–2607 (1999).
15. P. B. Johnson and R. W. Christy, "Optical constants of the noble metals," Phys. Rev. B **6**, 4370–4379 (1972).
16. U. Kreibig and C. v. Fragstein, "The limitation of electron mean free path in small silver particles," Z. Phys. **224**, 307–323 (1969).
17. J. P. Kottmann and O. J. F. Martin, "Accurate solution of the volume integral equation for high permittivity scatterers," IEEE Trans. Antennas Propag., in press (2000).
18. J. P. Kottmann, O. J. F. Martin, D. R. Smith and S. Schultz, "Dramatic localized electromagnetic enhancement in plasmon resonant nanoparticles," submitted to Phys. Rev. Lett. (2000).

1. Introduction

Small metal particles are known to exhibit resonant behavior at optical wavelengths. The extremely large electromagnetic field enhancements associated with these plasmon resonances are of great importance for nanoscience: In surface enhanced Raman scattering (SERS) [2,3] they play a key role in the amplification of the Raman signal of molecules adsorbed on rough metal particles [4–7]. In near field optical microscopy, they can provide a strong, well-defined and localized light source to investigate subwavelength structures [8]. While metallic nanoparticles produced by standard techniques (e.g., colloidal or evaporation) can have a broad variety of shapes, an accurate and complete description of the electromagnetic modes associated with such particles has not been available [9,10]. Such a description is particularly relevant to forward our understanding of SERS, which appears to be critically dependent on the detailed shape, material composition and configuration of the underlying metal nanoparticles. As the electromagnetic field enhancements of scatterers with spherical shape cannot explain the experimentally observed enhancement factors in SERS, the study of particles with arbitrary shape, as well as clusters of interacting particles, is of great importance [11].

In this paper we study the plasmon resonances of metal particles in the 10−100 (nm) range. Special attention is focussed on this range for three reasons: First, it is known from the analytic solution that the field enhancement at resonance is maximized for spherical particles with diameters in this range; we assume (and will show) that this is also valid for non-spherical particles. Second, the experimentally observed enhancement in SERS is the largest for nanoparticle dimensions of this scale. Third, technology is now reaching the state where particles of this size can be produced in a controlled manner [12–14].

2. Model

The plasmon resonances of nanoparticles can be investigated using Maxwell's equations [11]. As metals exhibit frequency dispersion, the permittivity varies with wavelength. For metals such as silver and gold, the permittivity can assume negative values at optical frequency. The underlying microscopic mechanism that leads to this negative permittivity is the interaction of the electromagnetic field with the conduction electrons.

For specific negative values of the permittivity, which depend on the size and shape of the particle, an external electromagnetic field can produce a resonantly enhanced polarization, leading to large scattering cross sections (SCS) and large electromagnetic fields near the particle. These distinct resonances are known as the surface polariton modes, or plasmon resonances of the particle. As we will see, different bounding surfaces have a strong impact on these plasmon resonances.

Since our focus here is the influence of the surface on the plasmon resonances, we do not consider further the fundamental processes that give rise to the dispersion, but rather use experimental values as obtained by Johnson and Christie [15]. Silver particles in the

#21116 - $15.00 US Received April 14, 2000; Revised May 18, 2000

$10-100$ (nm) size range, as investigated in this study, are well described with the bulk permittivity [16]. It is only for particles smaller than 10 (nm) that electron scattering at the particle boundary impinges on the conduction electrons mean free path. This however hardly influences the real part of the permittivity for silver nanoparticles, even below 10 (nm), and only increases the imaginary part of epsilon [11,16].

We investigate two-dimensional (2D) silver scatterers, illuminated with a transverse electric (TE) wave, where the electric field component lies in the plane of the figures. (In the transverse magnetic (TM) case, where the magnetic field is in the plane, plasmon resonances are not excited.) A 2D structure corresponds to an infinitely long structure in the third (not shown) dimension.

For our numerical simulations we use a recently developed finite elements solution of the volume integral equation [17]. The key point is a new regularization scheme that ensures a very high accuracy. Such an accuracy is mandatory for studying resonances numerically, because at the resonance a small change of the system parameters leads to a large change in the system response. We refer the reader to Ref. [17], where this numerical technique is described in detail and its accuracy assessed. The scatterers presented here are discretized with several thousand triangular elements.

Nanoparticles with triangular cross-sections are an exemplary case of non-regular particles. Triangular particles are interesting as they exhibit several complex phenomena, including multiple plasmon resonances, a longitudinal (bulk) plasmon mode, and a very large and localized field enhancement at the sharp tips [18]. To more closely match realistic particles, as well as to avoid numerical difficulties, we rounded off each corner of a particle by 0.25 (nm). For different geometries, we show the SCS as a function of the wavelength between 300 (nm) and 600 (nm). Since the extreme near field is of specific importance for SERS, we present detailed color maps of the field amplitude versus excitation wavelength in movies, with the wavelength as "time axis". To ease comparison, the same color map for the field amplitude is used throughout the paper.

3. Results

Only the plasmon resonances for simple shapes like a cylindrical or elliptical particle have been studied in detail. To provide a common ground, we first consider a 20 (nm)$\times$10 (nm) elliptical profile. Such an ellipse has two resonances corresponding to the illumination directions along the major and minor axes. These resonances are shown in Fig. 1, where the SCS is given as a function of the wavelength for three different illumination directions. We see that the resonance at $\lambda = 331$ (nm) corresponds to the illumination direction perpendicular to the minor axis, whereas the larger resonance at $\lambda = 357$ (nm) corresponds to the illumination direction perpendicular to the major axis. For incidence

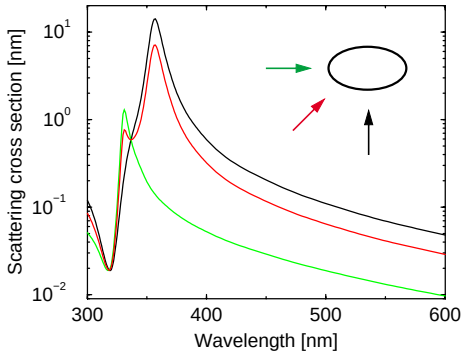

Fig. 1. SCS for an ellipse [overall size 20 (nm)$\times$10 (nm)]. Influence of the propagation direction.

#21116 - $15.00 US
Received April 14, 2000; Revised May 18, 2000

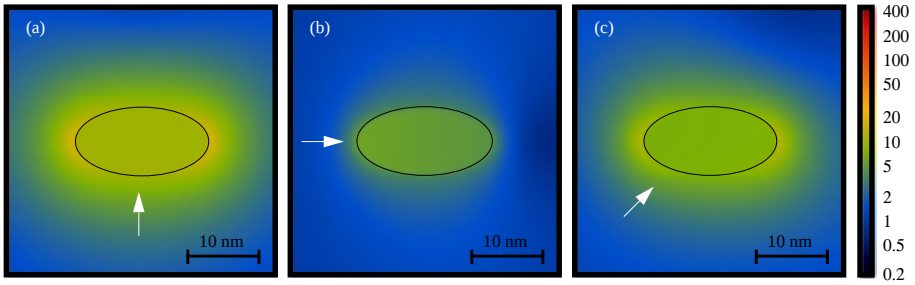

Fig. 2. Movies of the field amplitude distribution for a 20 (nm) × 10 (nm) ellipse illuminated along the (a) (01)–direction (609 KB), (b) (10)–direction (589 KB), (c) (11)–direction (606 KB) in the $\lambda = 300\,(\text{nm}) \ldots 600\,(\text{nm})$ wavelength range. Front pictures: (a) $\lambda = 357\,(\text{nm})$, (b) $\lambda = 331\,(\text{nm})$, (c) $\lambda = 357\,(\text{nm})$.

in a direction off either of the symmetry axes, both resonances are excited.

The movies Figs. 2(a)–(c) display the electromagnetic field amplitude distribution as a function of the wavelength, for three different illumination directions. The amplitude of the incident plane wave is one. At the resonances $\lambda = 331\,(\text{nm})$ and $\lambda = 357\,(\text{nm})$ the field distribution inside the ellipse is nearly constant, consistent with the well-known quasi-static result [11]. In the main resonance at $\lambda = 357\,(\text{nm})$ the field amplitude at close vicinity of the particle reaches 20 times that of the incident field. Note also that for oblique incidence the field distributions at the resonances [$\lambda = 331\,(\text{nm})$ and $\lambda = 357\,(\text{nm})$] are nearly symmetric with respect to the particle axes. This emphasizes the dominant role played by the resonances.

Figure 3 shows the SCS for a triangular particle, again for three different illumination directions. We observe a much more complex structure, with five distinct plasmon resonances that now cover a broader wavelength range, from 329 (nm) to 412 (nm).

As illustrated by the movies in Figs. 4(a)–(c), the field distributions associated with the triangle resonances have a much more complex structure. We observe local field enhancements of up to 200 in the main resonance at 412 (nm) [Fig. 4(a)]. An analysis of the field divergence shows that each mode is associated with a different surface polarization charge distribution. In the main resonance at 412 (nm) both corners have accumulated charge of different sign, oscillating within a period, whereas for the resonance at 365 (nm) both negative and positive charges are accumulated near each corner, which leads to a completely different field pattern with a more rapid decrease of the near field amplitude just outside of these corners.

Note also that, as for the ellipse, there is a particular illumination direction that max-

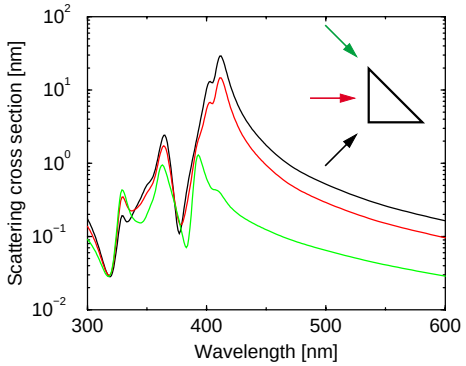

Fig. 3. SCS for a 20 (nm) base right angled isosceles triangular particle for three different incident direction.

#21116 - $15.00 US
Received April 14, 2000; Revised May 18, 2000

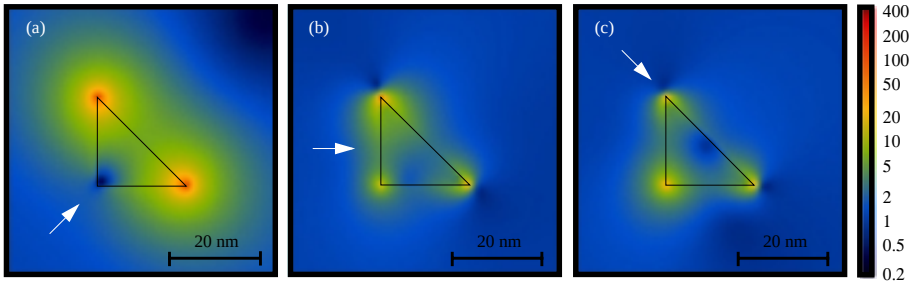

Fig. 4. Movies of the field amplitude distribution of the 20 (nm) triangular particle illuminated along the (a) (11)–direction (775 KB), (b) (10)–direction (772 KB), (c) $(1\overline{1})$–direction (758 KB) in the 300−600 (nm) wavelength range. Front pictures: (a) $\lambda = 412$ (nm), (b) $\lambda = 365$ (nm), (c) $\lambda = 363$ (nm).

imizes the excitation of each resonance. For example, the main resonance at 412 (nm) corresponds to the (11)–direction. Illuminating the particle at this wavelength from another direction leads to a reduction of intensity. Illumination perpendicular to this direction, as in the movie Fig. 4(c) at 412 (nm), does not lead to the excitation of this resonance.

Let us emphasize that this strong enhancement is not a lightening rod or tip effect, but truly a resonance related to the overall particle shape. Lightning rod effect, occurring when the particle is off-resonance, provides only a very small amplitude enhancement as illustrated by the movies in Figs. 4(a)–(c) for $\lambda = 300$ (nm).

Although not shown in this paper, there is a phase shift, up to approximately $\pi/4$ at the main resonance between the incident field and the scattered field near the particle. This phenomenon is well known from classical mechanics, where such a phase shift is observed when the driving frequency and the eigenfrequency of the system are close.

In Figure 5 we study the SCS of a right-angled isosceles triangle, illuminated along the (11)–direction, for different particle sizes. Two features, common also to spherical scatterers, are evident in these SCS plots: First, the red-shift of the resonances increases with increasing particle size, as can be clearly seen for the main resonance, located at 401 (nm) for the 10 (nm) base triangle, and 458 (nm) for the 100 (nm) particle. Second, the resonances broaden with increasing size with an accompanying decrease of the near field amplitude at the resonances. Although more resonances are excited for larger particles, the broadening leads to an overlapping of the resonances such that they cannot be resolved.

For the resonance at 329 (nm) however, we observe no red-shift. This is characteristic

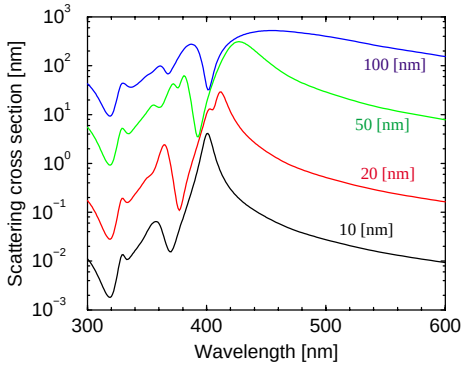

Fig. 5. SCS for right angled isosceles triangular particles illuminated along the (11)–direction. Four different particle sizes are investigated: 10, 20, 50 and 100 (nm) base.

#21116 - $15.00 US
Received April 14, 2000; Revised May 18, 2000

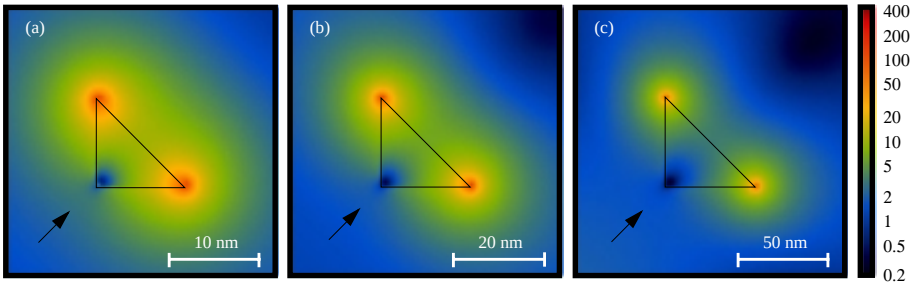

Fig. 6. Movies of the field amplitude distribution for right angled isosceles triangular particles illuminated along the (11)–direction with (a) 10 (nm) base (712 KB), (b) 20 (nm) base (775 KB), (c) 50 (nm) base (758 KB) in the 300−600 (nm) wavelength range. The front pictures represent the corresponding main resonance: (a) $\lambda = 401$ (nm), (b) $\lambda = 412$ (nm), (c) $\lambda = 427$ (nm).

of a longitudinal bulk mode (as opposed to a surface mode), the permittivity being close to zero at this wavelength. Moreover, this resonance exists for all incident directions [see Figs. 4(a)–4(c)], the field maxima being always located in a corner along the illumination direction. For the surface modes, on the other hand, the field maximum is located in a corner transverse to the illumination direction.

In the movies Figs. 6(a)–6(c) we see that with increasing size the near field amplitude decreases (as the resonance width increases), and that the field is more localized towards the surface of the triangle, as material losses become more important.

In Fig. 7 the SCS is shown for a 10 (nm) base, 20 (nm) perpendicular right angled triangle. Note the much more complex resonances for such a particle with low symmetry. These resonances extend over a broader wavelength range, the main resonance being obtained at $\lambda = 458$ (nm).

For (11) incidence, the field in the main resonance at 458 (nm) has extremely large values at the "sharp" corner where it reaches up to 400 times the incident amplitude [Fig. 8(a)]. In this mode, charge accumulates in the sharp corner, whereas the same charge amount of different sign is distributed over the remaining particle surface. Note also that in this main resonance the sharp corner acts like a point source, producing a radial field distribution in its vicinity, with a slow decrease of the field amplitude ($\approx 1/r$). Even at a distance of 10 (nm) from the sharp corner, the near field amplitude is still more than 10 times the incident amplitude.

For the resonance at 392 (nm) we obtain a similar large field enhancement at the sharp corner, however decreasing rapidly outside the particle, like for the resonance of the 20 (nm) triangle at $\lambda = 365$ (nm) [Fig. 4(a)]. Both negative and positive charges

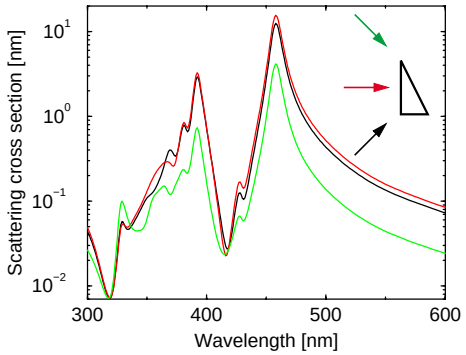

Fig. 7. SCS for a 10 (nm) base, 20 (nm) perpendicular right angled triangle for three different incident directions.

#21116 - $15.00 US
Received April 14, 2000; Revised May 18, 2000

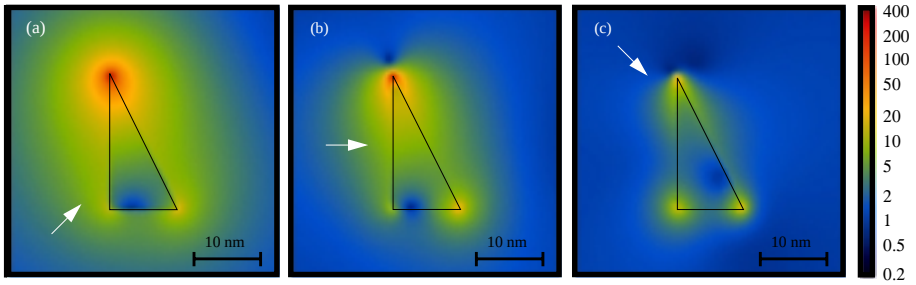

Fig. 8. Movies of the field amplitude distribution of the 10 (nm) base, 20 (nm) perpendicular right angled triangular particle illuminated along the (a) (11)–direction (966 KB), (b) (10)–direction (967 KB), (c) $(1\overline{1})$–direction (947 KB). Front pictures: (a) $\lambda = 458$ (nm), (b) $\lambda = 392$ (nm), (c) $\lambda = 364$ (nm), movies: (a)–(c): $\lambda = 300$ (nm)...600 (nm).

are accumulated near the corner, leading to a dipole-like field behavior in its vicinity, similar to the resonance of the 20 (nm) triangle at $\lambda = 365$ (nm) [Fig. 4(a)].

Again, we observe the weak resonance at 329 (nm) for all three directions of incidence, corresponding to the bulk mode.

3. Conclusions

Using a triangular particle as our model system, we have shown that non-spherical metal nanoparticles have a very complex behavior at optical wavelengths, with multiple resonances. These resonances crucially depend on the size and shape of the subwavelength nanoparticle. We observed that the field amplitudes associated with these resonances can be extremely large, up to several hundred times the incoming field amplitude. Furthermore, these large electromagnetic fields are strongly localized at particular positions on the particle surface. Such strong fields can explain the large enhancement factors observed experimentally in SERS, where the Raman signal is proportional – to a first approximation – to the fourth power of the electromagnetic amplitude enhancement. Simulations of the plasmon resonances for non-spherical particles can provide useful guidelines for different areas of nanoscience where extremely large electromagnetic fields – eventually at different wavelengths – are required.

Acknowledgments

The authors thank J.M. Favre and M. Paulus for their help with data visualization. This work was supported by the Swiss National Science Foundation, by the U.S.A. NSF (DBI-98-76651 and DMR-96-23949) and by the U.S.A. NIH (HG01959-02).